

BandEI: A Flexible Electrical Impedance Sensing Bandage for Deep Muscles and Tendons

Hongrui Wu*

University of Washington
Seattle, USA
hrwu@uw.edu

JaeYoung Moon

Gwangju Institute of Science and
Technology
Gwangju, Korea
super_moon@gm.gist.ac.kr

Feier Long*

University of Washington
Seattle, USA
feier513@uw.edu

Junyi Zhu†

University of Michigan
Ann Arbor, USA
zhujunyi@umich.edu

Hongyu Mao

University of Washington
Seattle, USA
hongyuum@uw.edu

Yiyue Luo†

University of Washington
Seattle, USA
yiyueluo@uw.edu



Figure 1: Users design customized, flexible BandEI patches via (a) an interactive UI, rapidly fabricate them, and seamlessly apply to various body parts (e.g., (b) ankle, (c) neck, and (d) wrist) for non-invasive electrical impedance sensing.

Abstract

Monitoring deep muscles and tissues is critical for rehabilitation, training, and fine motor control. In this work, we propose BandEI, a flexible, bandage-like wearable sensor for electrical impedance sensing. BandEI utilizes woven conductive fabric as the core material for its electrodes and leverages digital fabrication, including laser cutting, to enable scalable and customizable fabrication. To streamline the design process, we provide a user interface that allows users to freely select the deployment location of BandEI. The interface automatically generates fabrication-ready design files that accommodate for the curvature and shape of the selected area. We evaluate BandEI and validate its ability to detect signals from actively engaged large muscles, such as the biceps and triceps. Additionally, it can capture signals from deep or passively activated muscles, like those in the hand, which are typically difficult to detect with conventional surface electromyography (sEMG). We design and implement BandEI for muscles in the fingers, neck, and ankle, demonstrating its capability for diverse applications, including real-time gesture recognition, neck motion monitoring, and gait tracking.

*Co-first authors, equal contribution.

†Co-last authors, equal contribution.



This work is licensed under a Creative Commons Attribution 4.0 International License.

UIST '25, Busan, Republic of Korea

© 2025 Copyright held by the owner/author(s).

ACM ISBN 979-8-4007-2037-6/2025/09

<https://doi.org/10.1145/3746059.3747732>

CCS Concepts

- Human-centered computing → Interactive systems and tools.

Keywords

Fabrication, Sensors, Touch/Haptic/Pointing/Gesture

ACM Reference Format:

Hongrui Wu, Feier Long, Hongyu Mao, JaeYoung Moon, Junyi Zhu, and Yiyue Luo. 2025. BandEI: A Flexible Electrical Impedance Sensing Bandage for Deep Muscles and Tendons. In *The 38th Annual ACM Symposium on User Interface Software and Technology (UIST '25), September 28–October 1, 2025, Busan, Republic of Korea*. ACM, New York, NY, USA, 12 pages. <https://doi.org/10.1145/3746059.3747732>

1 INTRODUCTION

Humans rely on muscle activity for a vast range of physical tasks, from delicate movements like writing and manipulating small objects to more substantial actions such as lifting, running, and jumping. Understanding and measuring muscle activity is essential across various fields, including biomechanics [29, 31], rehabilitation [19, 35, 36], and human-computer interaction [17, 21, 37].

Various techniques have been developed to monitor muscle activity in different muscle groups. Surface electromyography (sEMG) measures electrical signals generated during active muscle contractions. It has been widely adopted to monitor large muscle group, such as triceps and quadriceps, for rehabilitation [19], sports performance optimization [29], and human-machine interaction [9, 10]. More recently, active sensing approaches, particularly electrical

Table 1: Comparison of muscle sensing modalities in terms of invasiveness, ability to sense small muscle groups, detection of tension/contraction/relaxation states, on-skin comfort, and space for related works.

Representative Study	Modality	Non-Invasiveness	Small Muscle Sensing	Tension	Contraction	Relaxation	On-Skin Comfort
Kotov-Smolenskiy <i>et al.</i> [19]	sEMG	✓	✗	✓	✓	✗	✓
Menkes and Pierce [23]	iEMG	✗	✓	✓	✓	✗	✗
EIT Kit [37]	EIT	✓	✗	✓	✓	✓	✓
Xu <i>et al.</i> [31]	EIM	✓	✗	✗	✗	✓	✓
BandEI (Ours)	El sensing	✓	✓	✓	✓	✓	✓

impedance-based techniques like electrical impedance tomography (EIT) and myography (EIM), have emerged as powerful alternatives. By injecting small currents and measuring the electrical impedance along the path, these techniques offer valuable insights into muscle activation, tendon movement, and physiological states. Electrical impedance sensing has demonstrated applications in muscle rehabilitation [35, 36], sports health care [31], and interactive systems [37].

While there has been significant success in monitoring large muscle groups, deep muscle groups remain difficult to assess due to their deeper location, more complex structure, and smaller size. Yet, these muscles are equally important, particularly for applications that require fine motor control, including diagnosing neuromuscular disorders, monitoring rehabilitation progress, and detecting micro gestures for interactive interfaces. Several studies have attempted to measure deep muscle activity in the hand [17], foot [25], or neck [20]. However, many studies infer deep muscle activity indirectly by measuring signals from nearby larger muscle groups, for example, detecting hand gestures through forearm muscle activity [1, 4, 21, 28, 33, 34]. More direct monitoring of deep muscles often relies on invasive methods, such as needle electromyography [23]. Achieving accurate, real-time, and non-invasive sensing in deep muscle groups requires active, flexible, and conformal sensing interfaces that can effectively access and measure activity from deep-seated structures.

In this paper, we propose BandEI, a flexible electrical impedance sensing system that enables customized sensor designs for deep muscles and tendons monitoring. By leveraging digital fabrication techniques, we expand the applicability of electrical impedance sensors to smaller, more complex anatomical regions. Our approach focuses on improving electrode placement precision, electrical stability, and user comfort, allowing for more effective monitoring of various body parts that were previously challenging for conventional EMG and EIT systems. Moreover, our solution is comprised of economical materials, facilitating straightforward prototyping and reproducibility of the system at a low cost.

We evaluate BandEI through two experiments. First, we compared our system with standard sEMG in high-intensity and low-intensity muscle contractions. The results indicate that BandEI not only captures subtle movements of small muscle groups (such as hands and neck) but also performs better than EMG in some low-force scenarios. Second, we validate that by placing BandEI directly on the hand and fingers we can detect subtle movements that are more difficult to identify when sensed from the wrist. It highlights the sensitivity, effectiveness, and versatility of BandEI. We showcase the capability of BandEI in three applications, including gesture recognition, neck posture tracking, and gait monitoring.

Our contributions are as follows:

- A bandage-like flexible electrical impedance sensing interface for deep muscle and tendons monitoring.
- A interactive design toolkit for customizing sensing layouts.
- A low-cost digital fabrication pipeline for creating customized conformal electrode arrays.
- Evaluation of our system for muscle activity monitoring.
- Demonstration of applications in deep muscles monitoring at ankle, neck, and fingers.

2 RELATED WORK

This work improves electrical impedance-based sensing for muscle activity by detecting signals from deep muscle groups and designing sensors that adapt to different body anatomies. To contextualize our research, we examine prior work in two key areas: muscle activity sensing in HCI, and digital design and fabrication for wearable physiological interfaces.

2.1 Muscle Activity Sensing in HCI

Muscle activity sensing is vital in HCI, with common techniques including Electromyography (EMG), Electrical Impedance Tomography (EIT), and Electrical Impedance Myography (EIM) (Table 1). EMG captures electrical signals from muscle activation, while EIT and EIM detect conductivity changes due to muscle contractions [6, 11]. These methods are widely used in rehabilitation [19, 35–37], sports analytics [29, 31], exoskeleton control [9, 10], and gesture recognition [1, 4, 21, 28, 33, 34].

In rehabilitation, sEMG and impedance-based sensors monitor muscle recovery and assist with exoskeleton control [19, 35, 36]. Sports applications use these tools to analyze muscle activation and health [29, 31]. For gesture recognition, both EMG and impedance-based techniques track forearm muscle activity to support VR, smart home, and mobile interfaces [1, 4, 21, 28, 33, 34].

However, sensing small or deep muscles remains difficult due to challenges in electrode placement, signal interference, and sensor size. While efforts exist to measure activity in fingers [17], feet [25], and neck [20], most systems target larger muscles. Invasive EMG (iEMG) is often needed for precise small-muscle measurements [23]. To address these limitations, we introduce a customizable fabrication pipeline for impedance-sensing electrodes tailored to small muscles and complex anatomies.

2.2 Digital Design and Fabrication for Interactive Interfaces

Fabrication technologies play a crucial role in Human-Computer Interaction (HCI) by enabling novel interaction paradigms through

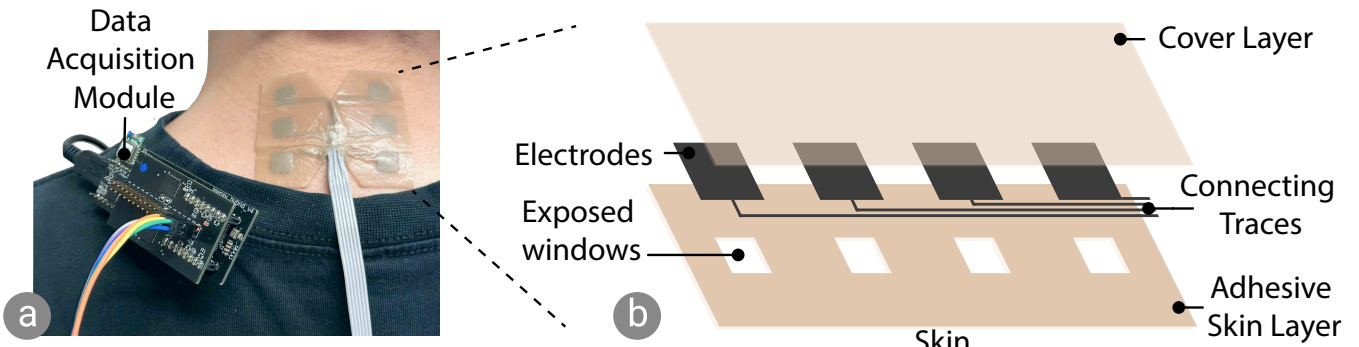


Figure 2: BandEI Overview. (a) The electrical impedance sensing patch is applied to the neck and connected to an impedance measurement circuit. (b) Exploded view of the BandEI three-layer structure: skin layer, conductive layer, and cover layer.

customized material properties and structures. Traditional fabrication methods have been continuously improved to enhance flexibility, scalability, and accessibility. Recent advancements in fabrication techniques such as laser cutting [3, 7, 15, 16, 26], multi-layering [7, 13, 18, 27], and conductive gel [8, 32] have allowed for more interactive and adaptive user interfaces.

Laser cutting is widely used in HCI for rapid prototyping and custom circuit fabrication. Systems like LaserFactory [26] and LaCir [7] automate circuit creation and simplify electronic prototyping for non-experts. Laser cutting enables precise, accessible fabrication of interactive electronics, particularly valuable for iterative design in HCI.

Multi-layering techniques enable flexible, interactive materials beyond rigid electronics. Glauser *et al.* [13] use 3D-printed multi-layered structures for deformation-based input, while IntelliTex [27] embeds conductive traces in textiles to support gesture and touch sensing. Multi-layering enhances the functionality, durability, and responsiveness of interactive surfaces, supporting richer, more natural user interactions.

Conductive gels offer flexible, skin-friendly alternatives to rigid electrodes. Xue *et al.* [32] demonstrate hydrogels for enhanced physiological sensing, and recent work [8] introduces self-adhesive, ink-printed electrodes that boost signal quality by 88% and reduce stimulation current. Conductive gels improve user comfort and signal quality in wearable systems, making them ideal for continuous or body-integrated sensing.

Building on these advances, we present a customizable Electrical Impedance Sensing (EIS) fabrication pipeline that combines laser cutting, multi-layering, and conductive materials. By unifying these techniques, our approach supports adaptable, user-centric fabrication of EIS interfaces for diverse HCI applications.

3 SYSTEM OVERVIEW

BandEI leverages electrical impedance sensing, an active sensing technique that applies a small alternating current (AC) through electrodes and measures the resulting voltage. This allows the system to calculate impedance, which varies with tissue composition, motion, and deformation, making it well-suited for detecting subtle physiological and biomechanical changes.

BandEI consists of an interactive design pipeline, a flexible bandage-like interface created through digital fabrication, and an integrated readout circuit, which is built on the open-source EIT-kit [37], which supports battery power and wireless communication via a BLE module (Microchip RN4871).

3.1 Design Rationale

BandEI offers a flexible, low-cost, and customizable solution for deep muscle monitoring.

Flexibility. Inspired by the design of a Band-Aid, BandEI is designed as a flexible and conformal sensor patch with customized shapes and electrode placements. This design enables sensing access to deep muscles and tendons in body regions with complex geometries. The conformal bandage-like structure can be tightly wrapped around and adhere to a broad range of curved body parts such as the fingers, wrists, and neck, enabling comfortable wear and stable skin contact. Compared to conventional medical electrodes, BandEI offers the advantage of miniaturization, allowing multiple electrodes to be deployed in compact areas, such as on the fingers. The new form factor of BandEI enables the deployment of electrical impedance sensing in regions that were previously difficult to access.

Cost Effectiveness. BandEI is designed to be cost-effective by using inexpensive materials and a streamlined digital fabrication process via CO₂ laser cutting. This affordability and minimal manual labor requirements make it suitable for both reusable and disposable use cases, depending on the application context. Most of the material cost comes from silicone sheets and conductive fabric. A finger-sized BandEI (Figure 11a) costs around \$0.40, and a larger neck-sized BandEI (Figure 2a) costs around \$1.00.

Customization. BandEI also emphasizes customization, supporting diverse anatomical regions and sensing requirements. The number, shape, and layout of electrodes can be tailored to specific use cases. Users can easily edit and preview BandEI designs through an interactive design tool (Section 3.2). The generated design files, combined with the rapid digital fabrication process (Section 3.3), allow users to produce ready-to-use sensor patches quickly.

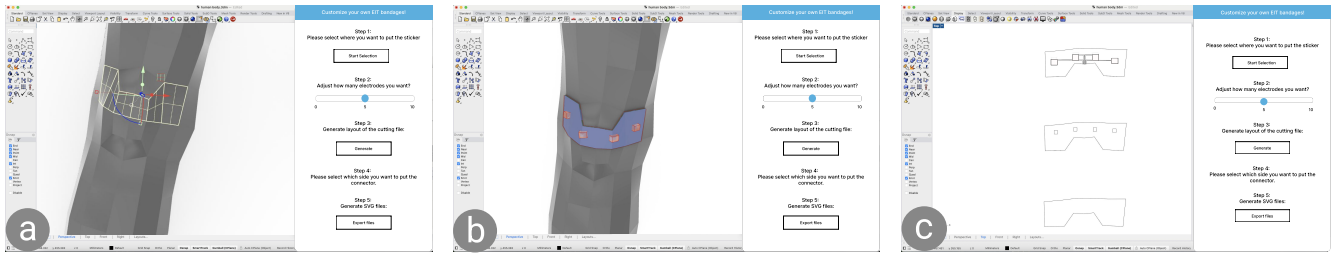


Figure 3: Design pipeline overview. (a) The user begins by selecting a 3D mesh model in the platform. (b) Our plugin then generates a preview of the personalized bandage design, (c) followed by the final layout for fabrication.

3.2 Interactive Design Pipeline

To support rapid prototyping and customization of a flexible electrical impedance sensing system, we develop an interactive 3D design interface (EI-Editor) (Figure 3) tailored for creating body-conforming bandages with customizable electrode distributions. Our tool enables users to define sensing regions directly on a 3D human mesh model and automatically generates a corresponding bandage-like geometry that ensures comfortable and tight contact with the body, accurate electrode placement, and seamless integration into a multi-layer fabrication pipeline.

Body-Conforming Bandage Generation. Users begin by selecting the desired sensing region on a 3D mesh model of the human body, which can be either imported from a scan or selected from a pre-existing library. EI-Editor analyzes the geometry of the selected mesh area and generates a corresponding 2d layout that closely conforms to the body surface. The system provides a real-time 3D preview to ensure the bandage fits the anatomical contour and aligns with user expectations.

Custom Electrode Placement. Within the editor, users can adjust the number, size, and spacing of electrodes, which are parameters that jointly influence sensing resolution, signal quality, and fabrication complexity. More electrodes and tighter spacing enable finer spatial sensing but increase design and wiring demands. Larger electrodes offer more stable signals but reduce resolution. The interface dynamically updates the preview to reflect changes, enabling real-time exploration of different sensing resolutions and layouts. Once finalized, the system generates a visualization of the complete multilayer bandage, including the conductive layer (electrode and wire layout), skin-contacting layer, and protective cover layer.

Fabrication File Generation. Once the design is complete, EI-Editor exports fabrication-ready files in the form of SVGs for each layer. These files are compatible with commercial laser cutters, enabling straightforward physical fabrication. Electrode shapes can be cut from conductive materials (e.g., silver-coated fabric), while the full bandage can be assembled by stacking the cut layers as shown in Figure 2b. This pipeline allows rapid iteration on bandage designs with minimal manual effort.

3.3 Fabrication

BandEI consists of three layers: an adhesive layer that contacts the skin, a middle layer containing conductive electrodes and connecting traces, and an outer protective cover (Figure 2). The electrodes

(8 mm × 8 mm) and connecting traces (1 mm width) are made from copper-nickel-plated woven conductive fabric (AMRADFIELD). Both the adhesive and cover layers are made of 0.4 mm thick medical-grade silicone sheets (MEDLOT). The adhesive layer includes 5 mm × 5 mm square openings to expose the electrodes for direct skin contact.

We develop a simple, repeatable fabrication pipeline for the multi-layer BandEI patches via laser cutting. The process includes five steps (Figure 4): laser cutting the skin and cover layers, laser cutting the conductive layer, soldering cable, assembling the layers, and applying the conductive gel. All three layers are precisely shaped using a CO₂ and fiber laser cutter (Figure 4a and b), with identical alignment frames included in the design to ensure accurate registration during assembly. Connection cables are soldered to the extended traces at the edge of the patch to establish reliable connectivity with the data acquisition system (Figure 4c). Soldering before assembly avoids exposing the silicone sheet to high temperatures, preventing potential damage. After that, the conductive electrodes and traces are transferred onto the adhesive layer, followed by placement of the cover layer (Figure 4d). Slightly over-sized electrode patches are used to tolerate minor misalignments and ensure consistent skin contact. Finally, conductive adhesive gel (TENSIVE) is then applied to the exposed electrodes. The gel fills the space between the skin and conductive patches and gradually solidifies to form a stable interface (Figure 4e).

4 RESULT

We evaluate the performance of the electrodes through impedance measurements and validate the effectiveness of electrical impedance sensing at the major muscles by using sEMG data as our baseline.

4.1 Impedance Characterization

We perform impedance measurements across a broad frequency range (100 Hz - 10 MHz) [14] to identify electrode materials and sizes that ensure stable performance and low-impedance skin contact.

Measurement Setup. As shown in Figure 5, we measure each electrode's impedance using a frequency response analysis (FRA) approach. The measurement setup consists a TL082 operational amplifier and a 1kΩ feedback resistor. A 1V peak-to-peak sinusoidal signal, sweeping from 100 Hz up to 10 MHz, is produced by an oscilloscope's function generator port, by using its built-in FRA module. The gain and phase responses between the input and output

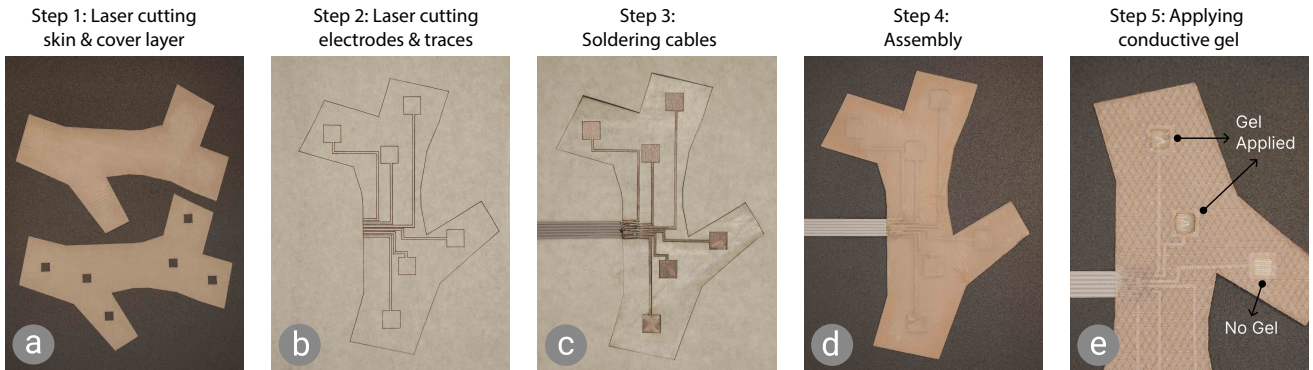


Figure 4: Fabrication pipeline of BandEI. The five-step process includes (a) laser cutting of skin and cover layer, (b) laser cutting on electrodes and connecting traces, (c) soldering, (d) layer assembly, and (e) application of conductive adhesive gel to enhance skin contact.

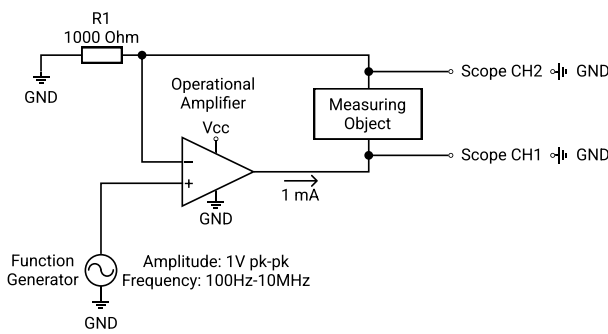


Figure 5: Circuit schematic for impedance characterization.

are obtained: Channel 1 (CH1) measures the input to the electrode, while Channel 2 (CH2) measures the output across the electrode. Using the measured gain and phase data, we calculate the complex impedance across the full frequency range.

Electrode Material Comparison. We evaluate the electrical impedance of different conductive materials, including commercial copper-nickel-plated woven conductive fabric, knitted conductive fabric, and copper tape (Figure 6a, 2-4), and compare it with a standard medical-grade Ag/AgCl gelled electrode (3M 2560, Figure 6a, 1). Figure 6b shows the measured impedance value across the bottom of the index finger for each material. The shaded regions indicate the standard deviation from measurements on six different participants.

Ag/AgCl electrodes, which have long been the standard for medical applications such as Electrocardiogram (ECG) and sEMG, serve as our benchmark for alternative electrode materials comparison. Both woven conductive fabric and knitted conductive fabric have lower impedance than Ag/AgCl across the entire frequency range. Notably, woven conductive fabric's impedance is nearly identical to that of Ag/AgCl in the low-to-mid frequency range, which is especially important for bio-impedance measurements. Although the knitted conductive fabric has slightly better electrical performance, its rough surface texture causes discomfort over long-time wearing. We also test electrodes made of copper tape, which similarly demonstrate low impedance. However, the rigidity of the copper

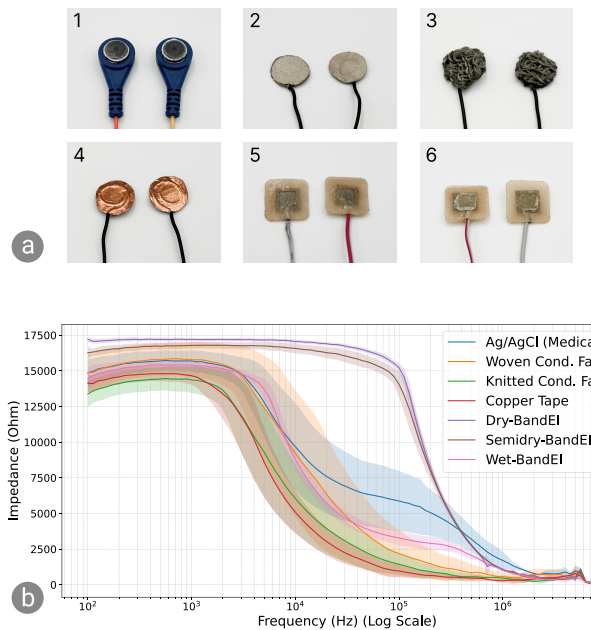


Figure 6: Comparison on Electrode Materials. (a) Six electrode types include Ag/AgCl, woven conductive fabric, knitted conductive fabric, copper tape, dry-BandEI, and semi-dry-BandEI. The wet-BandEI with a thin layer of conductive paste, shares the same appearance as (a.6) and is not shown. (b) Impedance-frequency characterization of each electrode type, showing their average impedance across a wide frequency range. Shaded areas represent standard deviation across multiple participants.

tape makes it not applicable for wearable applications. As a result, we choose woven conductive fabric as our final electrode material.

Conductive Gel and Paste. We then create band-aid-like prototypes by layering the selected woven conductive fabric as the middle

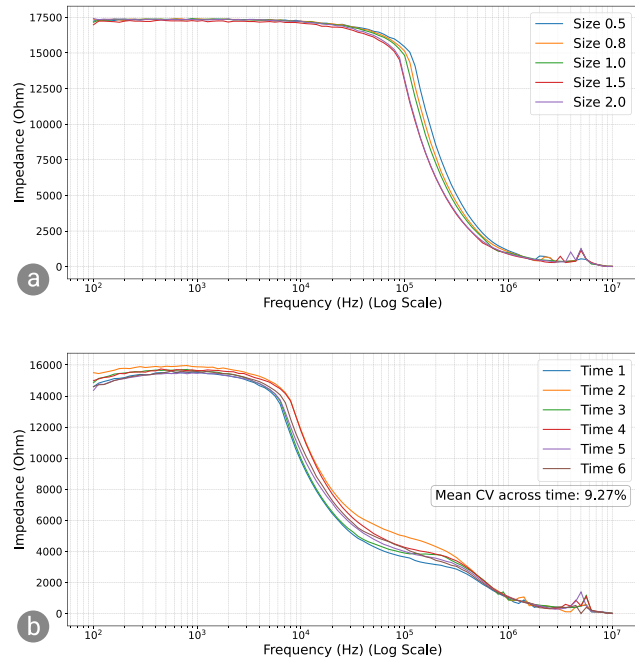


Figure 7: Impedance-frequency response of (a) electrodes of different sizes and (b) across time.

conductive layer. We further investigate the effect of conductive gel and paste by measuring the impedance over three different designs: dry-BandEI without conductive adhesive gel (TENSIVE) or conductive paste (TEN20), semi-dry-BandEI with conductive adhesive gel but without conductive paste, wet-BandEI with both conductive adhesive gel and conductive paste.

We find that the semi-dry-BandEI has slightly lower impedance than the dry-BandEI across the low-to-mid frequency range, and the wet-BandEI further reduces the impedance compared to the semi-dry-BandEI (Figure 6b). We observe that the conductive adhesive gel in the semi-dry-BandEI fills minor gaps caused by thickness mismatches between the electrodes and the skin at the exposed windows. It improves contact between the electrode and the skin. In wet-BandEI, the conductive paste further maintains surface moisture and a higher ion concentration, resulting in a more conductive skin-electrode interface. We use the wet-BandEI because of its high sensing performance and ease of fabrication. In the paper, all references to "BandEI" specifically refer to wet-BandEI electrodes using conductive adhesive gel and conductive paste.

Electrode Size Comparison. To identify the optimal electrode size, we fabricated electrodes in five different sizes ($5\text{ mm} \times 5\text{ mm}$, $8\text{ mm} \times 8\text{ mm}$, $10\text{ mm} \times 10\text{ mm}$, $15\text{ mm} \times 15\text{ mm}$, and $20\text{ mm} \times 20\text{ mm}$) using woven conductive fabric material. All electrodes were measured under the same conditions, where we place a pair of electrodes with a gap of 10 mm at the dorsal forearm. As shown in Figure 7a, smaller electrode sizes consistently result in higher impedance, with an approximately linear relationship observed in the low-to-mid frequency range. This trend aligns with our expectations, where larger contact areas provide lower impedance[14].

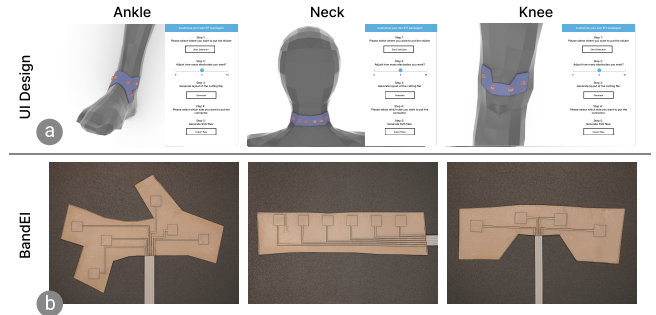


Figure 8: BandEI Prototypes. (a) The design and (b) fabricated prototypes of BandEI for three anatomical locations, including the ankle, neck, and knee.

Despite the lower impedance of larger electrodes, our target application requires compact, wearable electrodes that can be placed on small or curved body regions such as fingers. Therefore, we select the smallest tested size, $5\text{ mm} \times 5\text{ mm}$, as the final electrode dimension for our band-aid-like design.

Measurement across Time. To evaluate the stability of BandEI, we took repeated impedance measurements over a long period of time. Stability is a key characteristic of wearable electrodes, as they are often used and removed multiple times in real scenarios. In this experiment, electrical impedance was measured at six different time points. The first five measurements are taken at hours 0, 2, 4, 6, and 8 of the initial measurement, and the final measurement is taken at hour 24. At each time point, we reapplied conductive paste and reattached BandEI to simulate typical reuse scenarios. As shown in Figure 7b, all six electrical impedance curves exhibit highly similar shapes, indicating the consistency of impedance over time. The average coefficient of variation (CV) of bio-impedance across time is 9.27% for these six sets of data, which is acceptable [2].

4.2 Prototypes

We demonstrate prototypes of BandEI at the ankle, neck, and knee. All designs are achieved by our EI-Editor (Figure 8a). This user-friendly interface guides the user through each step of creating BandEI, from specifying electrode placements to finalizing the wearable's shape. By following on screen prompts, users can easily tailor and customize electrodes for any part of the body. The corresponding prototypes can be fabricated via laser cutting based on the exported design files. The customized BandEI prototypes demonstrate the adaptability and versatility of the system. Notably, for a typical BandEI, it only takes 10 minutes for the entire design and fabrication process. This significantly streamlines the creation of customized wearables interfaces.

4.3 Validation with EMG

sEMG is a well-established technique for assessing muscle activity and is regarded as the gold standard [12, 24, 30]. In this study, we use sEMG data as a reference benchmark to evaluate the electrical impedance sensing for muscle activity monitoring. By correlating

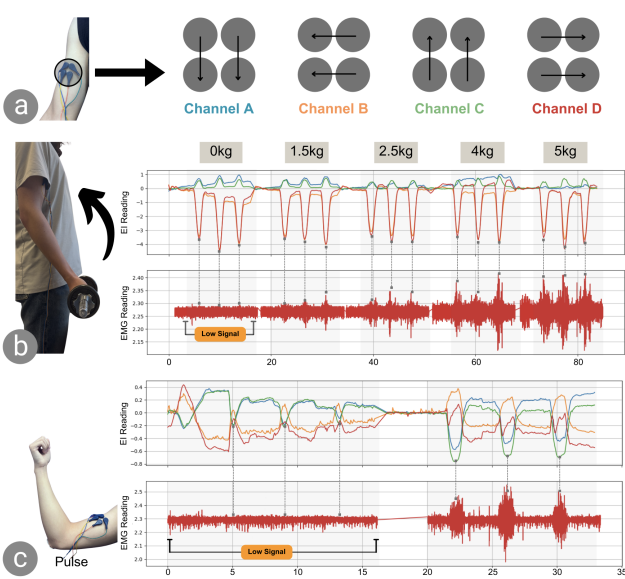


Figure 9: Validation with Dynamic Lifting Tasks. (a) Electrode orientation for bicep with four channels. (b) Dynamic Bending with incrementing weights mapped with both EI and EMG. (c) Dynamic Pulsing with minimal and maximum exerted force respectively.

electrical impedance signals with their corresponding sEMG recording across a range of dynamic and static tasks, our results consistently demonstrate strong alignment between these two modalities, thereby confirming the efficacy of electrical impedance for measuring muscle activity.

Figure 9a illustrates the electrode orientation and highlights four electrical impedance sensing channels, each obtained by altering the injection and receiving electrode pairs. In our validation, we employed commercial electrodes for both sEMG and electrical impedance sensing to ensure consistency and minimize variability stemming from electrode differences.

To evaluate the ability of electrical impedance sensing to capture both active and passive muscle states across different engagements, we design exercises that span dynamic and static conditions, with and without weights. For clarity in our experiments, dynamic tasks are defined as those involving a change in joint angle or muscle length (e.g., arm bending, transition between poses) whereas static tasks entail isometric contractions with no joint movement (e.g., isolated muscle pulses). This categorization provides a clear framework for examining electrical impedance sensing's performance under various contraction intensities and movement patterns.

As shown in Figure 10b, we measured synchronized sEMG and electrical impedance sensing data during incrementally weighted bending exercises (0 kg, 1.5 kg, 2.5 kg, 4 kg, and 5 kg). While electrical impedance sensing detects muscle activity for all weight conditions, sEMG failed to capture signals during unweighted contractions, as indicated by the bracket. This discrepancy can be attributed to sEMG's susceptibility to noise and its lower sensitivity

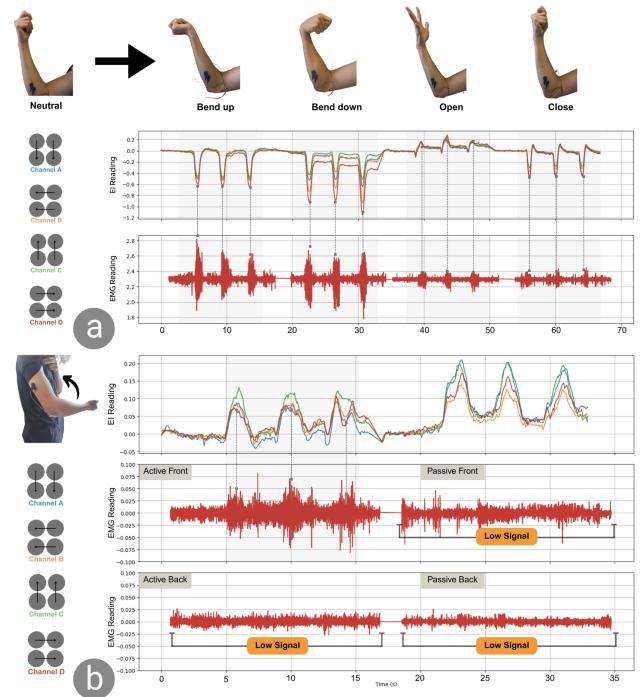


Figure 10: Validation with Pulsing Tasks and Passive Muscle Activation. (a) Various hand poses with their corresponding electrode orientation. (b) Dynamic Bending for Isometric and Isotonic Contraction Analysis.

when muscle activation is subtle. By contrast, electrical impedance sensing obtains higher sensitivity to changes in tissue, allowing it to register muscle activity across a broader range of forces, including very low-intensity contractions that are not detectable via sEMG.

We then measured for a series of static pulses at different force intensities, which further highlighted the electrical impedance sensing's sensitivity. Lighter pulses produce only low sEMG signals that are buried in noise, whereas electrical impedance sensing continues to provide clear indications of muscle engagement. In a subsequent set of dynamic exercises shown in Figure 10 (bend up, bend down, open, close), we compare electrical impedance sensing and sEMG signals with electrode placement repositioned to capture forearm muscle activity. Here, the electrical impedance sensing signal closely mirrors the pulse-to-pulse sEMG signal, emphasizing the versatility for tasks of varying muscle contraction levels.

Lastly, to validate electrical impedance sensing's potential for both active and passive muscle monitoring, we tested both isotonic and isometric contraction by placing electrodes over the biceps and triceps. During arm bending, the biceps actively contract, while the triceps experience passive lengthening (and vice versa during extension). In these scenarios, sEMG demonstrates limitations in detecting low-level signals while electrical impedance sensing consistently captures the subtle impedance changes that accompany both active and passive forces.

From these findings, it is evident that while sEMG remains the current gold standard for muscle activity monitoring, electrical

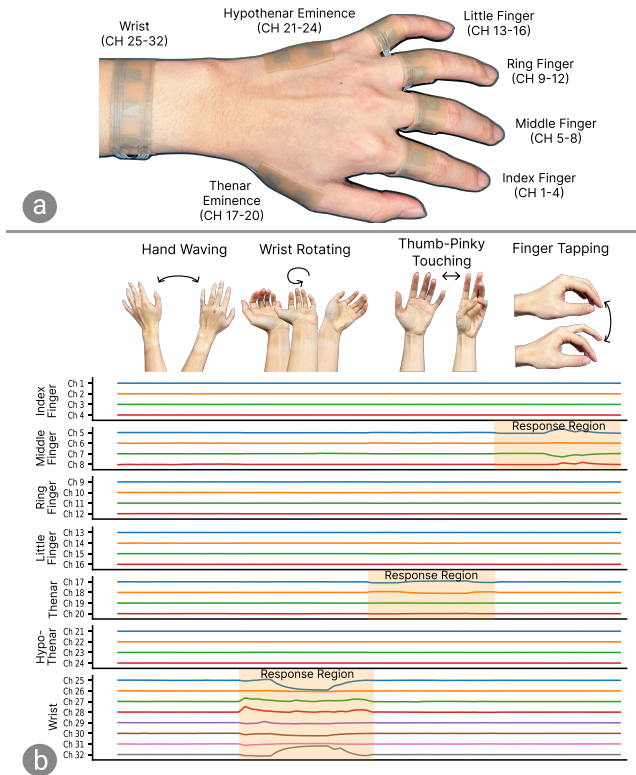


Figure 11: Validation with Wrist-worn Electrical Impedance Sensors. (a) BandEI placement on the hand, covering the wrist, thenar and hypothenar eminences, and individual fingers to enable localized muscle activity sensing. (b) Impedance signals from 32 BandEI channels during four gestures, showing region-specific responses corresponding to different muscle groups.

impedance sensing offers a powerful complementary modality. It not only supports sEMG data under conventional conditions but also expands detection capabilities to encompass more intricate, deep, or lower-force muscle activities that sEMG is often not able to capture. This enhanced sensitivity makes electrical impedance sensing a promising tool for applications where detailed muscle function monitoring is essential, and it has the potential to augment sEMG by capturing subtle or complex muscle movement beyond existing methods.

4.4 Validation with Wrist-worn Electrical Impedance Sensors

We further evaluate whether BandEI detects localized and subtle muscle or tendon activity that conventional wrist-worn electrical impedance sensing [21] often misses. While wrist-based impedance has demonstrated promising accuracy for gesture recognition, its sensing range is limited and may not capture fine-scale or region-specific actions, particularly those necessary for micro-gestures. To explore this limitation, we replicate existing wrist-based setups by collecting electrical impedance signals from both the wrist and

multiple regions of the hand, and then compare the respective responses across different anatomical sites.

We divide the hand into seven anatomically distinct regions: index finger, middle finger, ring finger, little finger, thenar eminence, hypothenar eminence, and wrist (Figure 11a). Each region is equipped with four electrodes, except for the wrist, which has eight, resulting in a total of 32 channels for interaction. To minimize crosstalk, our circuit activates only one electrode pair for current injection and another for voltage measurement per frame, with all other channels deactivated. This pair-by-pair activation ensures temporal isolation and minimizes crosstalk, with stable impedance acquisition at 30 frames per second with 32 channels. To evaluate this system, we select four diverse gestures to evaluate muscle engagement patterns: (1) Hand-waving; (2) Wrist Rotation; (3) Thumb-to-Pinky Touching; and (4) Finger Tapping. We choose these gestures not only for their biomechanical diversity but also because they represent well-established and distinguishable muscle activation patterns [22] [5].

Each gesture produces an electrical impedance signal that aligns with known anatomical function, as shown in Figure 11b: Hand waving shows negligible reactions in all regions, reflecting the limited involvement of hand and wrist muscles. Wrist rotation causes strong signal fluctuation only in the wrist area, whereas the hand channels remain nearly unchanged. Thumb-to-pinky touching generates clear responses in the thenar region that controls thumb movement. Finally, finger tapping (middle finger) appears most prominently on the middle finger channel, with minimal signals elsewhere.

These results indicate that BandEI is capable of capturing subtle, region-specific muscle activity that wrist-only setups may not be able to detect. Placing electrodes directly on the hand is crucial for observing such fine-grained signals; such capability broadens the scope of electrical impedance sensing and enables more detailed sensing of localized hand gestures in the future.

5 APPLICATION

We demonstrate BandEI in three applications, gesture recognition, head pose estimation, and gait monitoring, highlighting its ability to sense deep muscle activity across anatomically and functionally diverse regions.

5.1 Gestures and Micro-gestures Recognition

We demonstrate BandEI's ability to capture local deep muscle activity in the hand for gestures and micro-gestures recognition. The placement of the electrodes is consistent with the description in Section 4.4 and Figure 11a, in the hand area.

We collected data across a total of thirteen gestures [33], including: (1) four thumb-to-finger contact gestures (index through little), (2) four isolated micro finger lifts (excluding the thumb), and (3) five expressive gestures such as number six, thumbs up, claw, spiderman, and gun. Each gesture was recorded with 800 data samples and split into training, validation, and testing sets at a 60/20/20 ratio.

We trained a four-layer multi-layer perceptron (MLP) with ReLU activation functions to recognize these gestures, with an input of a 32, 24, 8, and 6-dimensional feature vector derived from the

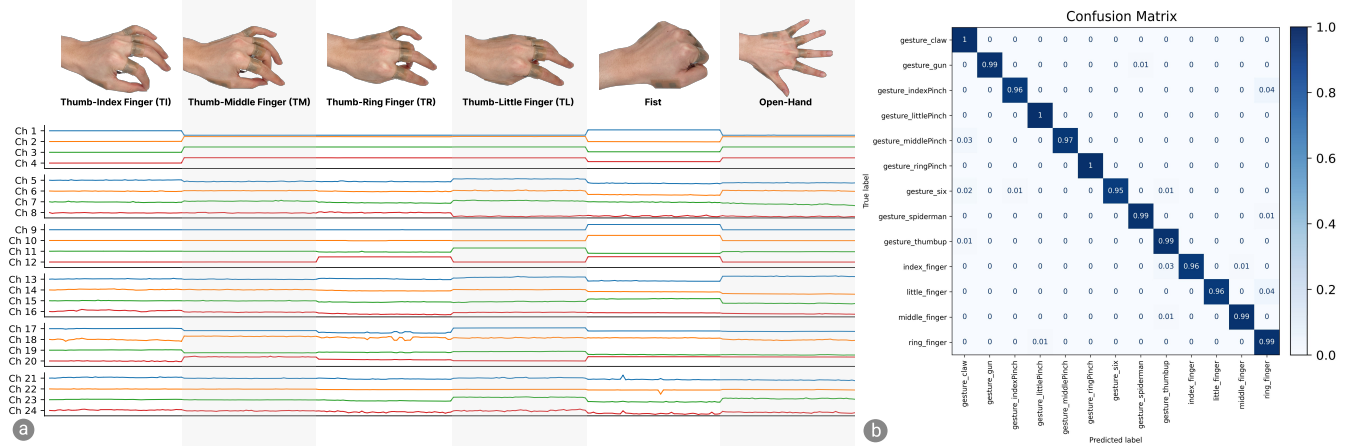


Figure 12: Gestures and Micro-gestures Recognition. (a) Example visualizations of electrical impedance patterns for four thumb-to-finger micro-gestures and two large-scale gestures (fist and open hand). (b) Confusion matrix showing classification performance across thirteen gestures, achieving 98% accuracy using BandEI.

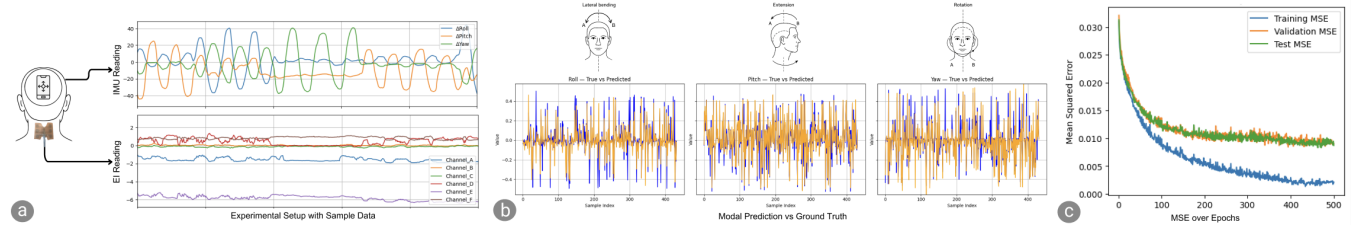


Figure 13: Head Pose Estimation. (a) Data collection set up and sample input (b) predicted output vs ground truth (c) MSE Per Epoch.

impedance readings of the 32 electrodes on the hand (Figure 11a). These input configurations correspond to all channels (32), finger-only (24), wrist-only (8), and a minimal finger setup (6), allowing us to evaluate the relative contribution of each region to classification performance.

As shown in the confusion matrix (Figure 12b), the finger-only model achieved 98% recognition accuracy across all thirteen types of gestures, indicating that BandEI can accurately capture small muscle activities under local hand attachment conditions and effectively distinguish different gesture actions.

To fairly compare signal richness across locations, we also varied the temporal context by testing multiple sliding window sizes (1, 5, and 10), holding the model architecture constant. In all settings, finger-based models consistently outperformed wrist-only models, which plateaued at 89% accuracy. Even with only six finger channels, the minimal configuration outperformed the complete wrist-based model, highlighting the superior spatial resolution and signal quality of the finger for fine motor intent.

5.2 Head Pose Estimation

In addition to the predominant study of the hand and wrist, we extend the capability of our BandEI platform to other anatomically and functionally significant regions of the body. We develop a custom six-channel electrode array, allowing for volumetric sensitivity,

potentially capturing subtle changes in muscle activation that are difficult to monitor using conventional techniques.

Traditional head-tracking methods, such as camera-based motion capture often require external setup. In contrast, our Electrical Impedance Sensing-based approach provides a wearable interface that is portable and operates in the wild. This enables real-time measurement of impedance variation to capture subtle muscle changes in the neck and makes it particularly suitable for scenarios where continuous monitoring is crucial.

To obtain ground-truth pose data alongside electrical impedance sensing signals, the participant wears both the six-channel neck electrode array and a custom head-mounted gyroscope (Figure 13a). Each data collection session lasted 60 seconds, during which the participant performed isolated roll, pitch, or yaw movements, as well as randomized sequences combining all three. Throughout all sessions, a total of 2,157 samples were collected, representing a broad spectrum of neck positions in three degrees of freedom (3DoF) and providing a comprehensive data set for subsequent model development and performance evaluation.

A seven layer multilayer perceptron (MLP) regression model was used to map the six electrical impedance sensing channels to three continuous orientation variables: roll, pitch, and yaw in Figure 13b. To facilitate the assessment, the dataset is split into 80%, 10%, 10% for training, validation, and testing respectively.

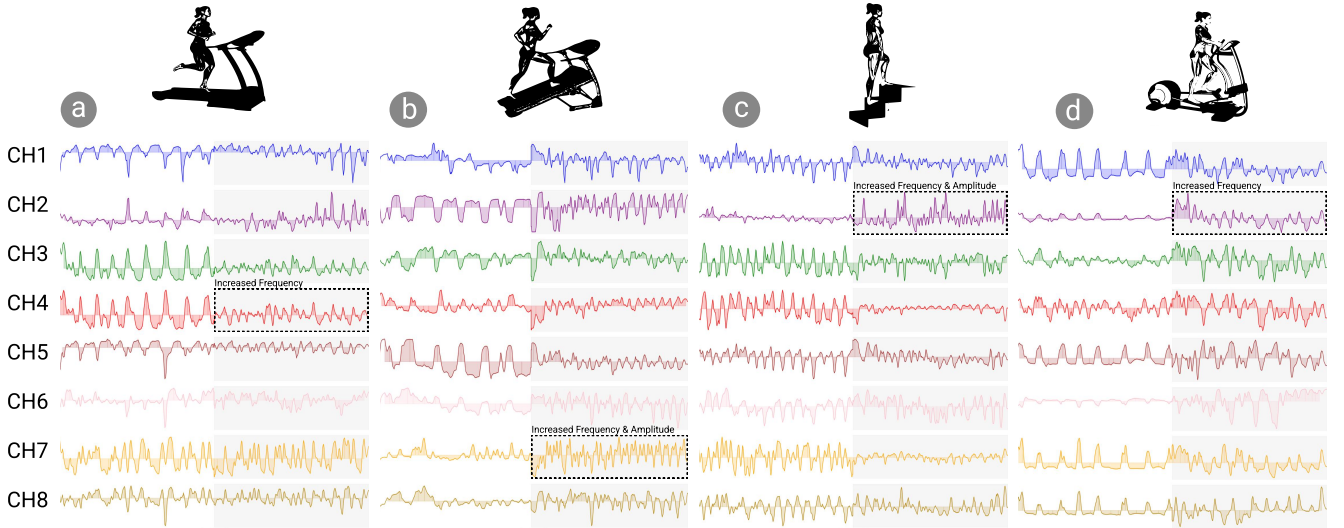


Figure 14: Electrical Impedance Signals Comparison with Different Gym Machines and Metrics. (a) Treadmill in flat condition with increasing BPM. (b) Treadmill in inclined condition with increasing BPM. (c) StairMaster with increasing intensity. (d) Elliptical with increasing speed.

We use Mean Square Error to quantify the model's accuracy shown in Figure 13c and Pearson correlation coefficient to quantify the strength of the linear relationship between the predicted values and the true values. Pitch exhibits the highest Pearson correlation coefficient at $r = 0.90$, potentially due to the relatively isolated nature of the nodding motion. Roll follows closely with $r = 0.87$, likely for the same hypothesis. Yaw, which involves a broader rotation across multiple muscle groups, shows an $r = 0.83$, suggesting that more complex movement may yield slightly lower correlations. Nevertheless, these results collectively indicate strong predictive capability for all three axes.

These results demonstrate the feasibility of BandEI to monitor neck movements across multiple degrees of freedom, offering a volumetric, high-sensitivity approach that capitalizes on the system's multi-channel designs and flexible electrode configuration.

5.3 Gait Monitoring

Monitoring muscle activity at the ankle presents unique challenges due to the joint's complex geometry and high degrees of freedom. To explore how BandEI can address these challenges, we design and fabricate an eight-electrode array that conforms to the curvature of the ankle, enabling a richer, multi-channel perspective of deep muscular and soft tissue changes.

We observe the performance of this ankle-mounted BandEI system during controlled exercise trials on three commonly used gym machines: a treadmill, a stair-climbing machine (StairMaster), and an elliptical trainer. On the treadmill, the participant walked and ran under both flat(level) and inclined conditions to target distinct muscle activation patterns. Each exercise session was structured to increase the level of exertion in discrete steps, through variations in speed, beats per minute(BPM), or resistance intensity. For clarity in comparison, we highlight the first and last phases of each trial, representing lower and higher exertion levels, respectively.

Figure 14 displays electrical impedance signals recorded from all eight channels for each exercise modality. The shaded region in the plot indicates a transition from the baseline to elevated intensity. Notably, multiple channels exhibit pronounced shifts in impedance amplitude and waveform patterns following these transitions, reflecting the heightened muscle engagement that occurs at higher workload levels(some example channels are marked with rectangles). These observations suggest that BandEI can capture dynamic fluctuation in muscular activity, reflecting changes in both exercise intensity and movement frequency at the ankle.

6 LIMITATION AND FUTURE WORK

BandEI demonstrates strong potential as a low-cost, rapidly customizable platform for electrical impedance sensing. Its ability to conform to various body regions, support high-density layouts, and maintain consistent signal quality across multiple sessions highlights its suitability for both prototyping and real-world physiological monitoring. The combination of digital fabrication and widely available materials enables quick iteration and affordable production, making it accessible to a wide range of users and use cases. Despite these advantages, several limitations remain that open important avenues for future exploration. In this section, we discuss key challenges related to signal interpretability, mechanical reliability, and customization interface flexibility, along with strategies for addressing them in future work.

Signal Interpretability. A fundamental limitation of electrical impedance sensing lies in the interpretability of its signals. Impedance varies with tissue composition, electrode placement, and anatomy, making it challenging to infer physiological states directly. To improve robustness and insight, future work will explore combining impedance sensing with surface electromyography (sEMG), leveraging Electrical Impedance Tomography(EIT)'s spatial resolution and EMG's temporal precision for a more interpretable hybrid system.

Mechanical Reliability and Skin Contact. Although BandEI is designed for low-cost, single-use scenarios, our experiments demonstrated that it remains reliable over multiple uses. We reused the same patch in over five data acquisition sessions (2 hours each) across two months. These results suggest that the materials and fabrication process offer sufficient durability for repeated research use. However, mechanical reliability during long-term or active wear remains a challenge. Specifically, BandEI is susceptible to electrode “floating” or partial detachment under heavy sweating or when applied to highly contoured surfaces. These conditions can disrupt skin contact and introduce signal instability. To mitigate this, we customize the bandage contour to match the geometry of the body region, minimizing edge lift and improving conformal fit. However, this solution is not always sufficient. Future iterations may incorporate breathable adhesives, sweat-resistant materials, or integrated mechanical supports to improve skin contact across diverse conditions. Improving this mechanical reliability will be especially important for longer-term deployment or high-motion tasks.

Fabrication and Customization. BandEI includes a digital design interface that supports rapid, user-driven customization of patch layouts. Users can configure key parameters such as the bandage contour, number of electrodes, electrode size, and inter-electrode spacing. Combined with a digital fabrication process and low-cost, widely available materials, this enables fast iteration and affordable production; each patch costs approximately \$1 in materials. However, we acknowledge that access to fabrication tools such as laser cutters may not be universal. Our cost estimation reflects material expenses only. In the current implementation, electrodes are dynamically and evenly distributed along the user-defined bandage contour to ensure balanced coverage and signal uniformity for general-purpose EIT sensing. While effective for most scenarios, this layout approach is based on geometric rules and does not account for anatomy-specific sensing goals or non-uniform sensitivity requirements. To address this, future versions of the interface will incorporate algorithmic layout strategies informed by anatomical landmarks or simulation feedback (e.g., EIT). Such improvements could enable more precise and personalized electrode configurations, particularly for high-resolution or task-specific applications.

7 CONCLUSION

We present **BandEI**, a flexible electrical impedance sensing system tailored for monitoring deep muscles and tendons in small or anatomical complex regions. By integrating digital fabrication, a customizable design tool, and low-cost materials, BandEI addresses multiple limitations of traditional muscle activity sensors, particularly in terms of electrode placement precision, signal stability, and user comfort. Our evaluations demonstrate BandEI’s capability to detect subtle, low-force muscle activity, especially in challenging areas such as the finger and neck, thereby enabling applications that include fine-grained gesture recognition, posture tracking, and gait monitoring.

A primary contribution of our work lies in the low-cost, reproducible fabrication pipeline and the interactive design toolkit, which empower users to rapidly prototype and adapt electrode layouts for specific anatomical targets. This modular approach

facilitate broader adoption in HCI, rehabilitation, and healthcare where custom-fit wearables are crucial for ensuring measurement accuracy and user comfort.

References

- [1] Christoph Amma, Thomas Krings, Jonas Böer, and Tanja Schultz. 2015. Advancing Muscle-Computer Interfaces with High-Density Electromyography. In *Proceedings of the 33rd Annual ACM Conference on Human Factors in Computing Systems* (Seoul, Republic of Korea) (*CHI ’15*). Association for Computing Machinery, New York, NY, USA, 929–938. <https://doi.org/10.1145/2702123.2702501>
- [2] Shimon Aronhime, Claudia Calcagno, Guido H. Jajamovich, Hadrien Arezki Dyvorne, Philip Robson, Douglas Dieterich, M. Isabel Fiel, Valérie Martel-Laferrière, Manjul Chatterji, Henry Rusinek, and Bachir Taouli. 2014. DCE-MRI of the liver: Effect of linear and nonlinear conversions on hepatic perfusion quantification and reproducibility. *Journal of Magnetic Resonance Imaging* 40, 1 (2014), 90–98. <https://doi.org/10.1002/jmri.24341> arXiv:<https://onlinelibrary.wiley.com/doi/pdf/10.1002/jmri.24341>
- [3] Wedyan Babatian, Christine Park, Hiroshi Ishii, and Neil Gershenfeld. 2025. Laser-Enabled Fabrication of Flexible Printed Electronics with Integrated Functional Devices. *Advanced Science* n/a, n/a (2025), 2415272. <https://doi.org/10.1002/advs.202415272> arXiv:<https://advanced.onlinelibrary.wiley.com/doi/pdf/10.1002/advs.202415272>
- [4] Lorena Isabel Barona López, Francis M. Ferri, Jonathan Zea, Ángel Leonardo Valdivieso Caraguay, and Marco E. Benalcázar. 2024. CNN-LSTM and post-processing for EMG-based hand gesture recognition. *Intelligent Systems with Applications* 22 (2024), 200352. <https://doi.org/10.1016/j.iswa.2024.200352>
- [5] Marco E. Benalcázar, Cristhian Motoche, Jonathan A. Zea, Andrés G. Jaramillo, Carlos E. Anchundia, Patricio Zambrano, Marco Segura, Freddy Benalcázar Palacios, and María Pérez. 2017. Real-time hand gesture recognition using the Myo armband and muscle activity detection. In *2017 IEEE Second Ecuador Technical Chapters Meeting (ETCM)*, 1–6. <https://doi.org/10.1109/ETCM.2017.8247458>
- [6] Tushar Kanti Bera. 2018. Applications of Electrical Impedance Tomography (EIT): A Short Review. *IOP Conference Series: Materials Science and Engineering* 331, 1 (mar 2018), 012004. <https://doi.org/10.1088/1757-899X/331/1/012004>
- [7] Niels Christian Buch, Carlos Tejada, Daniel Ashbrook, and Valkyrie Savage. 2024. LaCir: A multilayered laser-cuttable material to co-fabricate circuitry and structural components. In *Proceedings of the 2024 CHI Conference on Human Factors in Computing Systems* (Honolulu, HI, USA) (*CHI ’24*). Association for Computing Machinery, New York, NY, USA, Article 340, 10 pages. <https://doi.org/10.1145/3613904.3642888>
- [8] Jia Xi Mary Chen, Tianhao Chen, Yixin Zhang, Weiqing Fang, Wenxuan Evelyn Li, Terek Li, Milos R. Popovic, and Hani E. Naguib. 2024. Conductive Bio-based Hydrogel for Wearable Electrodes via Direct Ink Writing on Skin. *Advanced Functional Materials* 34, 40 (2024), 2403721. <https://doi.org/10.1002/adfm.202403721> arXiv:<https://advanced.onlinelibrary.wiley.com/doi/pdf/10.1002/adfm.202403721>
- [9] Weihai Chen, Mingxing Lyu, Xilun Ding, Jianhua Wang, and Jianbin Zhang. 2023. Electromyography-controlled lower extremity exoskeleton to provide wearers flexibility in walking. *Biomedical Signal Processing and Control* 79 (2023), 104096. <https://doi.org/10.1016/j.bspc.2022.104096>
- [10] Ana Cisnal, Javier Pérez-Turiel, Juan-Carlos Fraile, David Sierra, and Eusebio de la Fuente. 2021. RobHand: A Hand Exoskeleton With Real-Time EMG-Driven Embedded Control. Quantifying Hand Gesture Recognition Delays for Bilateral Rehabilitation. *IEEE Access* 9 (2021), 137809–137823. <https://doi.org/10.1109/ACCESS.2021.3118281>
- [11] David Djajaputra. 2005. Electrical Impedance Tomography: Methods, History and Applications. *Medical Physics* 32, 8 (2005), 2731–2731. <https://doi.org/10.1118/1.1995712> arXiv:<https://aapm.onlinelibrary.wiley.com/doi/pdf/10.1118/1.1995712>
- [12] Scott Bateman Ethan Eddy, Erik J Scheme. 2023. A Framework and Call to Action for the Future Development of EMG-Based Input in HCI. In *CHI ’23: Proceedings of the 2023 CHI Conference on Human Factors in Computing Systems*.
- [13] Oliver Gläuser, Daniele Panozzo, Otmar Hilliges, and Olga Sorkine-Hornung. 2019. Deformation Capture via Soft and Stretchable Sensor Arrays. *ACM Trans. Graph.* 38, 2, Article 16 (March 2019), 16 pages. <https://doi.org/10.1145/3311972>
- [14] Sverre Grimnes and Ørjan G. Martinsen. 2000. *Bioimpedance and Bioelectricity Basics*. ELSEVIER, United Kingdom.
- [15] Daniel Groeger and Jürgen Steimle. 2019. LASEC: Instant Fabrication of Stretchable Circuits Using a Laser Cutter. In *Proceedings of the 2019 CHI Conference on Human Factors in Computing Systems* (Glasgow, Scotland UK) (*CHI ’19*). Association for Computing Machinery, New York, NY, USA, 1–14. <https://doi.org/10.1145/3290605.3300929>
- [16] Tao Han, Anindya Nag, Nasrin Afsharimanesh, Subhas Chandra Mukhopadhyay, Sudip Kundu, and Yongzhao Xu. 2019. Laser-Assisted Printed Flexible Sensors: A Review. *Sensors* 19, 6 (2019). <https://doi.org/10.3390/s19061462>
- [17] Xuhui Hu, Aiguo Song, Jianzhi Wang, Hong Zeng, and Wentao Wei. 2022. Finger movement recognition via high-density electromyography of intrinsic and extrinsic hand muscles. *Scientific Data* 9, 1 (2022), 373. <https://doi.org/10.1038/s41597-022-01402-w>

- 022-01484-2
- [18] Haoqiang Hua, Wei Tang, Xiangmin Xu, David Dagan Feng, and Lin Shu. 2019. Flexible Multi-Layer Semi-Dry Electrode for Scalp EEG Measurements at Hairy Sites. *Micromachines* 10, 8 (2019). <https://doi.org/10.3390/mi10080518>
 - [19] AM Kotov-Smolenskiy, AE Khizhnikova, AS Klochkov, NA Suponova, and MA Piradov. 2021. Surface EMG: applicability in the motion analysis and opportunities for practical rehabilitation. *Human Physiology* 47, 2 (2021), 237–247. <https://doi.org/10.1134/S0362119721020043>
 - [20] Simon Krasna and Srdan Đorđević. 2020. Estimating the Effects of Awareness on Neck-Muscle Loading in Frontal Impacts with EMG and MC Sensors. *Sensors* 20, 14 (2020). <https://doi.org/10.3390/s20143942>
 - [21] Alexander Kyu, Hongyu Mao, Junyi Zhu, Mayank Goel, and Karan Ahuja. 2024. EITPose: Wearable and Practical Electrical Impedance Tomography for Continuous Hand Pose Estimation. In *Proceedings of the 2024 CHI Conference on Human Factors in Computing Systems* (Honolulu, HI, USA) (CHI '24). Association for Computing Machinery, New York, NY, USA, Article 402, 10 pages. <https://doi.org/10.1145/3613904.3642663>
 - [22] Jaime E. Lara, Leo K. Cheng, Oliver Röhrle, and Niranchan Paskaranandavadiwel. 2022. Muscle-Specific High-Density Electromyography Arrays for Hand Gesture Classification. *IEEE Transactions on Biomedical Engineering* 69, 5 (2022), 1758–1766. <https://doi.org/10.1109/TBME.2021.3131297>
 - [23] Daniel L. Menkes and Robert Pierce. 2019. Needle EMG muscle identification: A systematic approach to needle EMG examination. *Clinical Neurophysiology Practice* 4 (2019), 199–211. <https://doi.org/10.1016/j.cnp.2019.08.003>
 - [24] Michael S. Eggleston, Mingde Zheng, Michael S. Crouch. 2022. Surface Electromyography as a Natural Human–Machine Interface: A Review. *IEEE Sensors Journal* (2022).
 - [25] Kamila Mortka, Agnieszka Wiertel-Krawczuk, and Przemysław Lisiński. 2020. Muscle Activity Detectors—Surface Electromyography in the Evaluation of Abductor Hallucis Muscle. *Sensors* 20, 8 (2020). <https://doi.org/10.3390/s20082162>
 - [26] Martin Nisser, Christina Chen Liao, Yuchen Chai, Aradhana Adhikari, Steve Hodges, and Stefanie Mueller. 2021. LaserFactory: A Laser Cutter-based Electromechanical Assembly and Fabrication Platform to Make Functional Devices & Robots. In *Proceedings of the 2021 CHI Conference on Human Factors in Computing Systems* (Yokohama, Japan) (CHI '21). Association for Computing Machinery, New York, NY, USA, Article 663, 15 pages. <https://doi.org/10.1145/3411764.3445692>
 - [27] Yuecheng Peng, Danchang Yan, Haotian Chen, Yue Yang, Ye Tao, Weitao Song, Lingyun Sun, and Guanyun Wang. 2024. IntelliTex: Fabricating Low-cost and Washable Functional Textiles using A Double-coating Process. In *Proceedings of the 2024 CHI Conference on Human Factors in Computing Systems* (Honolulu, HI, USA) (CHI '24). Association for Computing Machinery, New York, NY, USA, Article 859, 18 pages. <https://doi.org/10.1145/3613904.3642759>
 - [28] Jinxian Qi, Guozhang Jiang, Gongfa Li, Ying Sun, and Bo Tao. 2019. Intelligent Human–Computer Interaction Based on Surface EMG Gesture Recognition. *IEEE Access* 7 (2019), 61378–61387. <https://doi.org/10.1109/ACCESS.2019.2914728>
 - [29] Juri Taborri, Justin Keogh, Anton Kos, Alessandro Santuz, Anton Umek, Caryn Urbanczyk, Eline van der Kruk, and Stefano Rossi. 2020. Sport Biomechanics Applications Using Inertial, Force, and EMG Sensors: A Literature Overview. *Applied Bionics and Biomechanics* 2020, 1 (2020), 2041549. <https://doi.org/10.1155/2020/2041549> arXiv:<https://onlinelibrary.wiley.com/doi/pdf/10.1155/2020/2041549>
 - [30] Murat Zinnuroğlu veysel Alcan. 2023. Current developments in surface electromyography. *Turkish journal of medical sciences* (2023).
 - [31] Pan Xu, Junwei Zhou, Zhizhang David Chen, Xudong Yang, Hongli Yan, Željka Lučev Vasić, Mario Cifrek, Sio Hang Pun, Mang I Vai, and Yueming Gao. 2024. Advancements and Challenges in Electrical Impedance Myography (EIM): A Comprehensive Overview of Technology Development, Applications in Sports Health, and Future Directions. *IEEE Journal of Microwaves* 4, 4 (2024), 605–625. <https://doi.org/10.1109/JMW.2024.3427710>
 - [32] Hailing Xue, Dongyang Wang, Mingyan Jin, Hanbing Gao, Xuhui Wang, Long Xia, Dong'ang Li, Kai Sun, Huanan Wang, Xufeng Dong, et al. 2023. Hydrogel electrodes with conductive and substrate-adhesive layers for noninvasive long-term EEG acquisition. *Microsystems & Nanoengineering* 9, 1 (2023), 79. <https://doi.org/10.1038/s41378-023-00524-0>
 - [33] Yang Zhang and Chris Harrison. 2015. Tomo: Wearable, Low-Cost Electrical Impedance Tomography for Hand Gesture Recognition. In *Proceedings of the 28th Annual ACM Symposium on User Interface Software & Technology* (Charlotte, NC, USA) (UIST '15). Association for Computing Machinery, New York, NY, USA, 167–173. <https://doi.org/10.1145/2807442.2807480>
 - [34] Yang Zhang, Robert Xiao, and Chris Harrison. 2016. Advancing Hand Gesture Recognition with High Resolution Electrical Impedance Tomography. In *Proceedings of the 29th Annual Symposium on User Interface Software and Technology* (Tokyo, Japan) (UIST '16). Association for Computing Machinery, New York, NY, USA, 843–850. <https://doi.org/10.1145/2984511.2984574>
 - [35] Junyi Zhu, Yuxuan Lei, Aashini Shah, Gila Schein, Hamid Ghaednia, Joseph Schwab, Casper Harteveld, and Stefanie Mueller. 2022. Monitoring Muscle Engagement via Electrical Impedance Tomography for Unsupervised Physical Rehabilitation. In *Adjunct Proceedings of the 35th Annual ACM Symposium on User Interface Software and Technology* (Bend, OR, USA) (UIST '22 Adjunct). Association for Computing Machinery, New York, NY, USA, Article 110, 3 pages. <https://doi.org/10.1145/3526114.3558633>
 - [36] Junyi Zhu, Yuxuan Lei, Aashini Shah, Gila Schein, Hamid Ghaednia, Joseph Schwab, Casper Harteveld, and Stefanie Mueller. 2022. MuscleRehab: Improving Unsupervised Physical Rehabilitation by Monitoring and Visualizing Muscle Engagement. In *Proceedings of the 35th Annual ACM Symposium on User Interface Software and Technology* (Bend, OR, USA) (UIST '22). Association for Computing Machinery, New York, NY, USA, Article 33, 14 pages. <https://doi.org/10.1145/3526113.3545705>
 - [37] Junyi Zhu, Jackson C Snowden, Joshua Verdejo, Emily Chen, Paul Zhang, Hamid Ghaednia, Joseph H Schwab, and Stefanie Mueller. 2021. EIT-Kit: An Electrical Impedance Tomography Toolkit for Health and Motion Sensing. In *The 34th Annual ACM Symposium on User Interface Software and Technology* (Virtual Event, USA) (UIST '21). Association for Computing Machinery, New York, NY, USA, 400–413. <https://doi.org/10.1145/3472749.3474758>